

Electronic Supplementary Information for

Conservation of the insert-2 motif confers Rev1 from different species with an ability to disrupt G-quadruplexes and stimulate translesion DNA synthesis

Amit Ketkar¹, Reham S. Sewilam¹, Mason J. McCrury¹, Jaycelyn S. Hall¹, Ashtyn Bell¹, Bethany C. Paxton¹, Shreyam Tripathi³, Julie E.C. Gunderson², and Robert L. Eoff^{1,*}

¹ Department of Biochemistry and Molecular Biology, University of Arkansas for Medical Sciences, Little Rock, AR 72205 USA

² Department of Physics, Hendrix College, Conway, AR 72032, USA

³ Arkansas School for Mathematics, Sciences, and the Arts, Hot Springs, AR 71901 USA

* To whom correspondence should be addressed. Tel: +1 501 686 8343; Fax: +1 501 686 8169; Email: RLEoff@uams.edu

Running title: G4 properties of Rev1 from different species

ELECTRONIC SUPPLEMENTARY INFORMATION

CONTENTS

Table S1. Equilibrium dissociation constants for Rev1 homologs binding to ss-G4 and non-G4 DNA substrates in a buffer containing 100 mM LiCl.

Table S2. Equilibrium dissociation constants for Rev1 homologs binding to primer/template (p/t)-G4 and non-G4 DNA substrates in a buffer containing 100 mM LiCl.

Table S3. Equilibrium dissociation constants for hRev1³³⁰⁻⁸³³ wild-type and E466A/Y470A mutant proteins binding to ss- and ds-G4 and non-G4 DNA substrates in a buffer containing 100 mM LiCl.

Figure S1. Purification of hRev1 wild-type and mutant proteins, as well as the Rev1 homologs.

Figure S2. Measurement of Rev1-catalyzed dCMP insertion on 13/42-mer DNA substrates.

Figure S3. Measurement of Rev1-catalyzed dCMP insertion on 23/42-mer DNA substrates.

Figure S4. Evaluation of different G4 substrates and the effect of protein storage buffer on results of the G4 hemin assay.

Figure S5. Binding curves for Rev1 homologs with G4 and non-G4 ssDNA substrates in 100 mM KCl buffer ($K_{D,DNA}$ values reported in **Table 2**).

Figure S6. Binding curves for Rev1 homologs with G4 and non-G4 p/t DNA substrates in 100 mM KCl buffer ($K_{D,DNA}$ values reported in **Table 3**).

Figure S7. Binding curves for Rev1 homologs with ss42-mer, 13/42-mer and 23/42-mer Myc G4 and non-G4 DNA substrates in 100 mM KCl buffer ($K_{D,DNA}$ values reported in **Table 4**).

Figure S8. Binding curves for hRev1³³⁰⁻⁸³³ E466A/Y470A with ss- and p/t- G4 and non-G4 DNA substrates in 100 mM KCl buffer ($K_{D,DNA}$ values reported in **Table 5**).

Figure S9. Binding curves for hRev1³³⁰⁻⁸³³ WT and hRev1³³⁰⁻⁸³³ E466A/Y470A with ss42-mer, 13/42-mer and 23/42-mer Myc G4 and non-G4 DNA substrates in 100 mM KCl buffer ($K_{D,DNA}$ values reported in **Table 6**).

Figure S10. Binding curves for Rev1 homologs with G4 and non-G4 ssDNA substrates in 100 mM LiCl buffer ($K_{D,DNA}$ values reported in **Table S1**).

Figure S11. Binding curves for Rev1 homologs with G4 and non-G4 p/t DNA substrates in 100 mM LiCl buffer ($K_{D,DNA}$ values reported in **Table S2**).

Figure S12. Binding curves for hRev1³³⁰⁻⁸³³ E466A/Y470A with ss- and p/t- G4 and non-G4 DNA substrates in 100 mM LiCl buffer ($K_{D,DNA}$ values reported in **Table S3**).

Table S1. Equilibrium dissociation constants for Rev1 homologs binding to ss-G4 and non-G4 DNA substrates in a buffer containing 100 mM LiCl^a.

	$K_{D,DNA}$		Fold preference for G4 DNA ($K_{D,NonG4\ DNA}/K_{D,G4\ DNA}$)
	Non-G4 (nM)	G4 (nM)	
yRev1 (a.a. 305-746)			
Myc 14/23	361 ± 73	286 ± 34	1.3
TBA	477 ± 82	405 ± 44	1.2
hTelo-4	418 ± 67	388 ± 54	1.1
IRev1 (a.a. 1-448)			
Myc 14/23	233 ± 24	167 ± 34	1.4
TBA	288 ± 32	225 ± 41	1.3
hTelo-4	466 ± 54	419 ± 26	1.1
zRev1 (a.a. 1-872)			
Myc 14/23	203 ± 23	57 ± 13	3.5
TBA	196 ± 43	98 ± 11	2
hTelo-4	143 ± 51	52 ± 17	2.8

^aFluorescence polarization experiments were performed by titrating each protein into a solution containing the indicated ss-DNA substrate containing 100 mM LiCl. The resulting equilibrium dissociation constant values were calculated by fitting the resulting polarization values to a quadratic equation. Data represent the mean ± std. dev. (n=3).

Table S2. Equilibrium dissociation constants for Rev1 homologs binding to p/t-G4 and non-G4 DNA substrates in a buffer containing 100 mM LiCl^a.

	$K_{D,DNA}$		Fold preference for G4 DNA ($K_{D,NonG4\ DNA}/K_{D,G4\ DNA}$)
	Non-G4 (nM)	G4 (nM)	
yRev1 (a.a. 305-746)			
Myc 14/23	398 ± 53	341 ± 44	1.2
TBA	541 ± 61	446 ± 37	1.2
hTelo-4	412 ± 63	367 ± 51	1.1
IRev1 (a.a. 1-448)			
Myc 14/23	411 ± 42	343 ± 41	1.2
TBA	623 ± 64	535 ± 72	1.2
hTelo-4	511 ± 68	452 ± 65	1.1
zRev1 (a.a. 1-872)			
Myc 14/23	227 ± 23	93 ± 16	2.4
TBA	249 ± 52	167 ± 25	1.5
hTelo-4	238 ± 58	107 ± 18	2.2

^a Data represent the mean ± std. dev. (n=3).

Table S3. Equilibrium dissociation constants for hRev1³³⁰⁻⁸³³ wild-type and E466A/Y470A binding to ss- and p/t-G4 and non-G4 DNA substrates in a buffer containing 100 mM LiCl^a.

	$K_{D,DNA}$		Fold preference for G4 DNA
	Non-G4 (nM)	G4 (nM)	$(K_{D,NonG4\ DNA}/K_{D,G4\ DNA})$
hRev1 (a.a. 330-833)			
ss-Myc-14/23*	760 ± 290	220 ± 70	4
p/t-Myc-14/23	817 ± 51	315 ± 45	2.6
ss-TBA*	310 ± 40	140 ± 20	2.2
p/t-TBA	415 ± 67	345 ± 90	1.2
ss-Telo-4*	920 ± 120	630 ± 100	1.5
p/t-Telo-4	976 ± 135	704 ± 110	1.4
hRev1 (a.a. 330-833)			
E466A/Y470A			
ss-Myc-14/23	832 ± 110	554 ± 120	1.5
p/t-Myc-14/23	876 ± 130	612 ± 140	1.4
ss-TBA	435 ± 125	346 ± 57	1.3
p/t-TBA	521 ± 120	404 ± 95	1.3
ss-Telo-4	1120 ± 200	946 ± 125	1.2
p/t-Telo-4	1230 ± 320	987 ± 180	1.3

^a Data represent the mean ± std. dev. (n=3).

*Values reproduced from earlier publication; Ketkar *et al*, *Nucleic Acids Res.* 2021 Feb 26;49(4) 2065-2084.

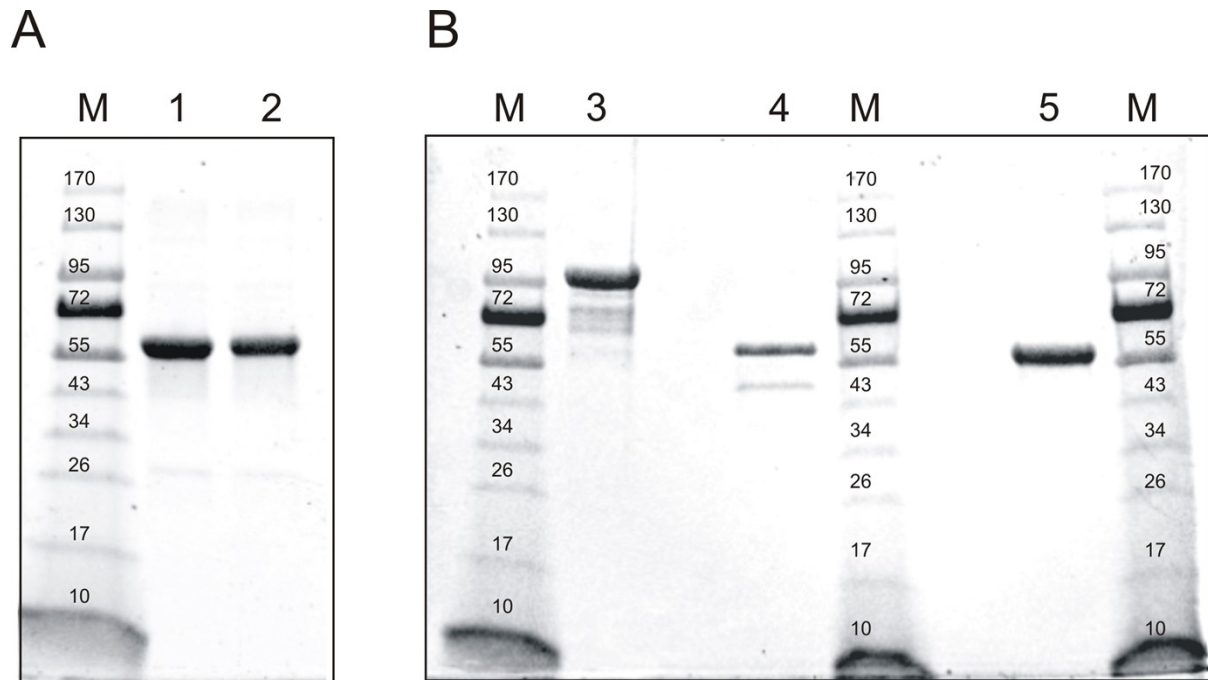


Figure S1. hRev1³³⁰⁻⁸³³ wild-type and mutant proteins, as well as the Rev1 homologs were overexpressed in *E. coli* BL21 (DE3) cells and purified to homogeneity, as described in the Materials and Methods section of the main text. We loaded 10 μ g of protein in each lane of a 4-20% gradient SDS-PAGE gel and bands were visualized by staining with Coomassie Brilliant Blue R-250. **A.** Lane 1, hRev1³³⁰⁻⁸³³ wild-type; lane 2, hRev1³³⁰⁻⁸³³ E466A/Y470A. **B.** Similar to A, the purified Rev1 homolog proteins were separated on a SDS-PAGE gel and visualized. Lane 3, zRev1¹⁻⁸⁶²; lane 4, yRev1³⁰⁵⁻⁷⁴⁶; lane 5, lRev1¹⁻⁴⁴⁸. In each lane M, 10 μ L of EZ-Run protein ladder (Thermo-Fisher) was loaded as reference.

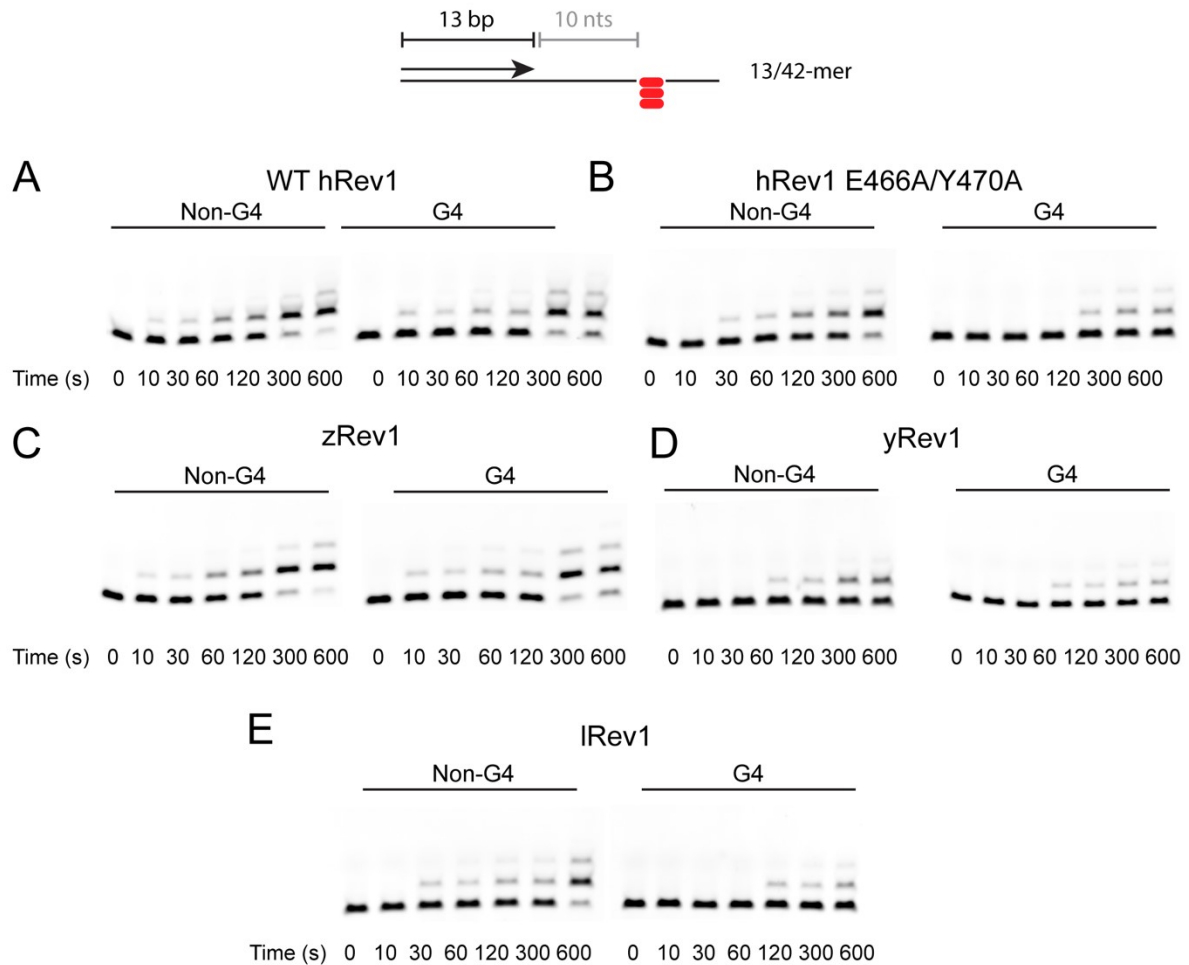


Figure S2. Measurement of Rev1-catalyzed dCMP insertion on 13/42-mer DNA substrates. The cytidyl transferase activity of Rev1 was measured by incubating enzyme (50 nM) with 13/42-mer DNA (200 nM), by annealing a FAM-labeled 13-mer primer to both the 42-mer G4 template derived from the Myc-14,23 sequence and the 42-mer non-G4-template (see Table 1 in main text for sequences). Nucleotide insertion was allowed to proceed for the indicated amounts of time before quenching with 95% (v/v) formamide, 20 mM EDTA, and 0.1% (w/v) bromophenol blue. Substrate and products were separated by denaturing polyacrylamide gel electrophoresis (7 M urea/14% w/v polyacrylamide). Results are shown for (A) WT hRev1³³⁰⁻⁸³³, (B) hRev1³³⁰⁻⁸³³ E466A/Y470A, (C) zRev1¹⁻⁸⁶², (D) yRev1³⁰⁵⁻⁷⁴⁶, and (E) IRev1¹⁻⁴⁴⁸.

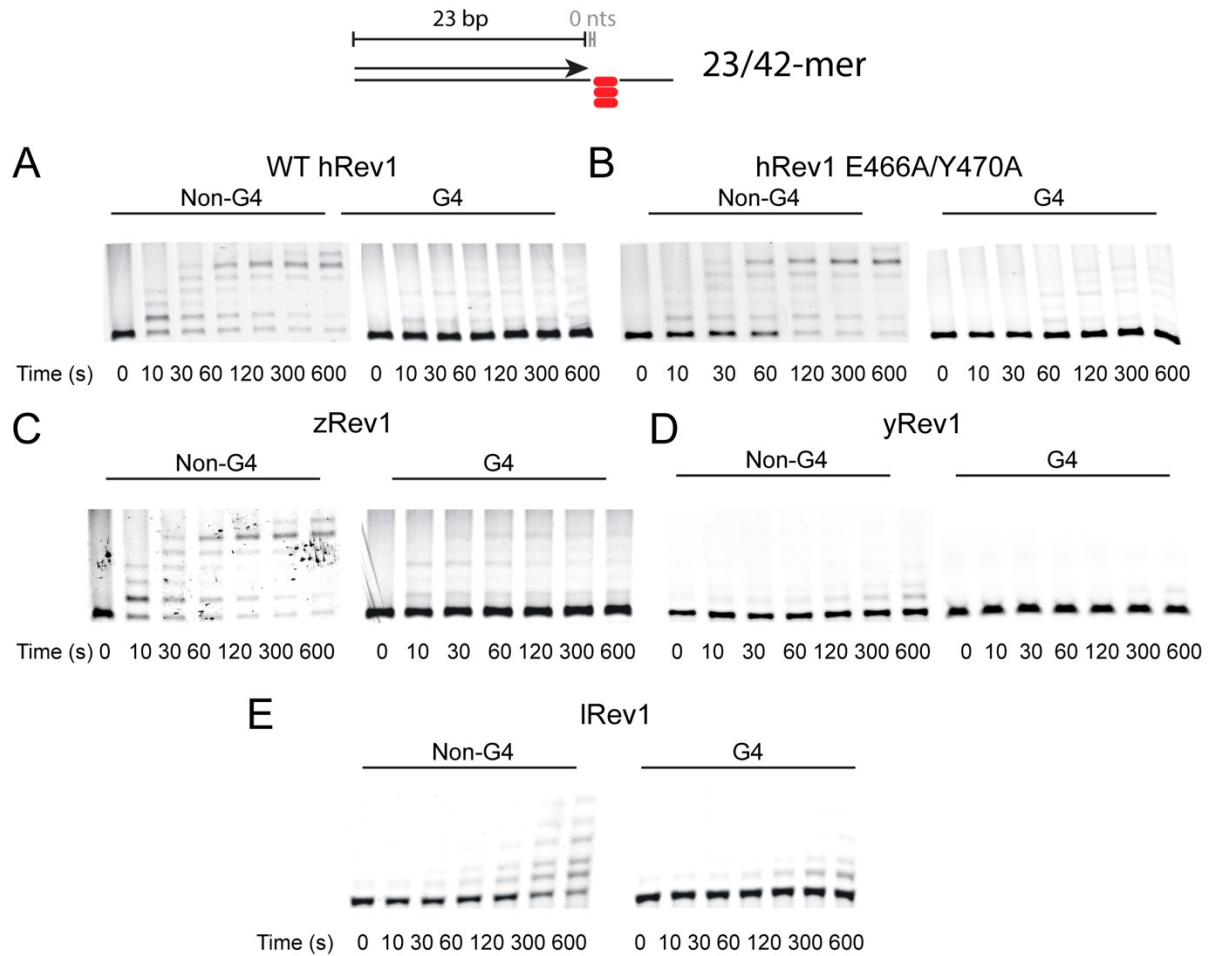


Figure S3. Measurement of Rev1-catalyzed dCMP insertion on 23/42-mer DNA substrates. The cytidyl transferase activity of Rev1 was measured by incubating enzyme (50 nM) with 23/42-mer DNA (200 nM), by annealing a FAM-labeled 23-mer primer to both the 42-mer G4 template derived from the Myc-14,23 sequence and the 42-mer non-G4-template (see Table 1 in main text for sequences). Nucleotide insertion was allowed to proceed for the indicated amounts of time before quenching with 95% (v/v) formamide, 20 mM EDTA, and 0.1% (w/v) bromophenol blue. Substrate and products were separated by denaturing polyacrylamide gel electrophoresis (7 M urea/14% w/v polyacrylamide). Results are shown for (A) WT hRev1³³⁰⁻⁸³³, (B) hRev1³³⁰⁻⁸³³ E466A/Y470A, (C) zRev1¹⁻⁸⁶², (D) yRev1³⁰⁵⁻⁷⁴⁶, and (E) IRev1¹⁻⁴⁴⁸.

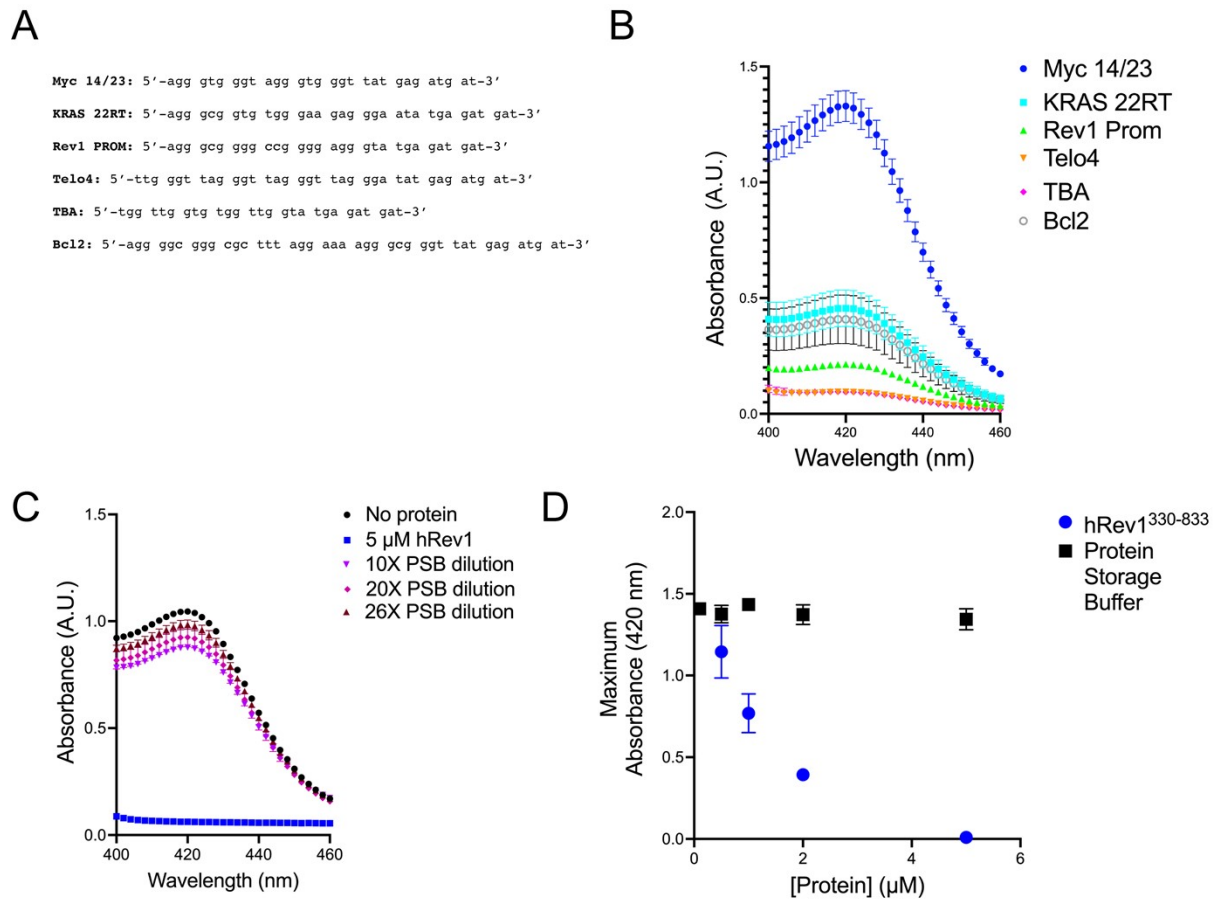


Figure S4. Evaluation of different G4 substrates and the effect of protein storage buffer on results of the G4 hemin assay. **A.** Sequences of different G4 substrates tested with the G4 hemin assay. **B.** Absorbance was measured for each of the ss-G4 DNA substrates (1 μ M) listed in panel A. **C.** To control for potential effects from protein storage buffer, we conducted the G4 hemin assay with ss-G4 DNA (Myc 14/23 42-mer, 1 μ M) adding either protein storage buffer (PSB) or WT hRev1 (5 μ M). The PSB was diluted 10X, 20X, or 26X. The 10X dilution involved adding 8 μ L of PSB into an 80 μ L total reaction volume and represents the maximal impact on G4 DNAzyme signal from PSB for experiments reported in this study. The 26X dilution corresponding to the same dilution factor used for the G4 hemin experiments where 5 μ M WT hRev1 was used. **D.** We repeated the G4 hemin assay with ss-G4 DNA (Myc 14/23 29-mer, 1 μ M), titrating in either WT hRev1 at the indicated concentrations or adding diluted PSB. The decrease in G4 DNAzyme signal was only observed when WT hRev1 was added to the reaction mixture.

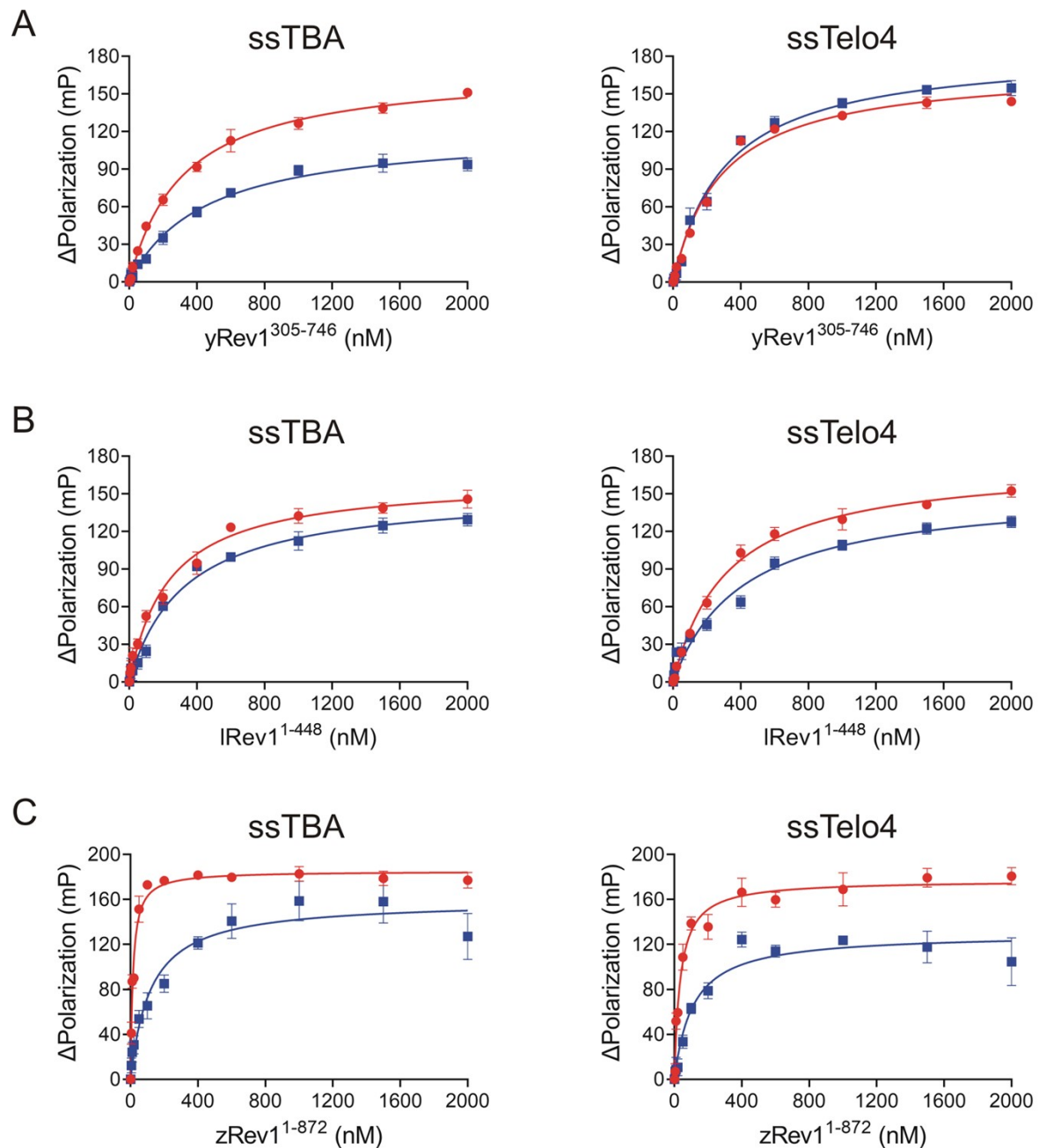


Figure S5. Binding curves for **A)** $yRev1^{305-746}$, **B)** $IRev1^{1-448}$ and **C)** $zRev1^{1-872}$ with the indicated G4 (red) or non-G4 (blue) ssDNA substrates in 100 mM KCl buffer. Proteins were titrated into a solution of each DNA (1 nM), and the change in fluorescence polarization at each protein concentration was measured and plotted as a function of concentration. The calculated $K_{D,DNA}$ values are listed in **Table 2**. The reported values represent the mean \pm std. dev. ($n=3$).

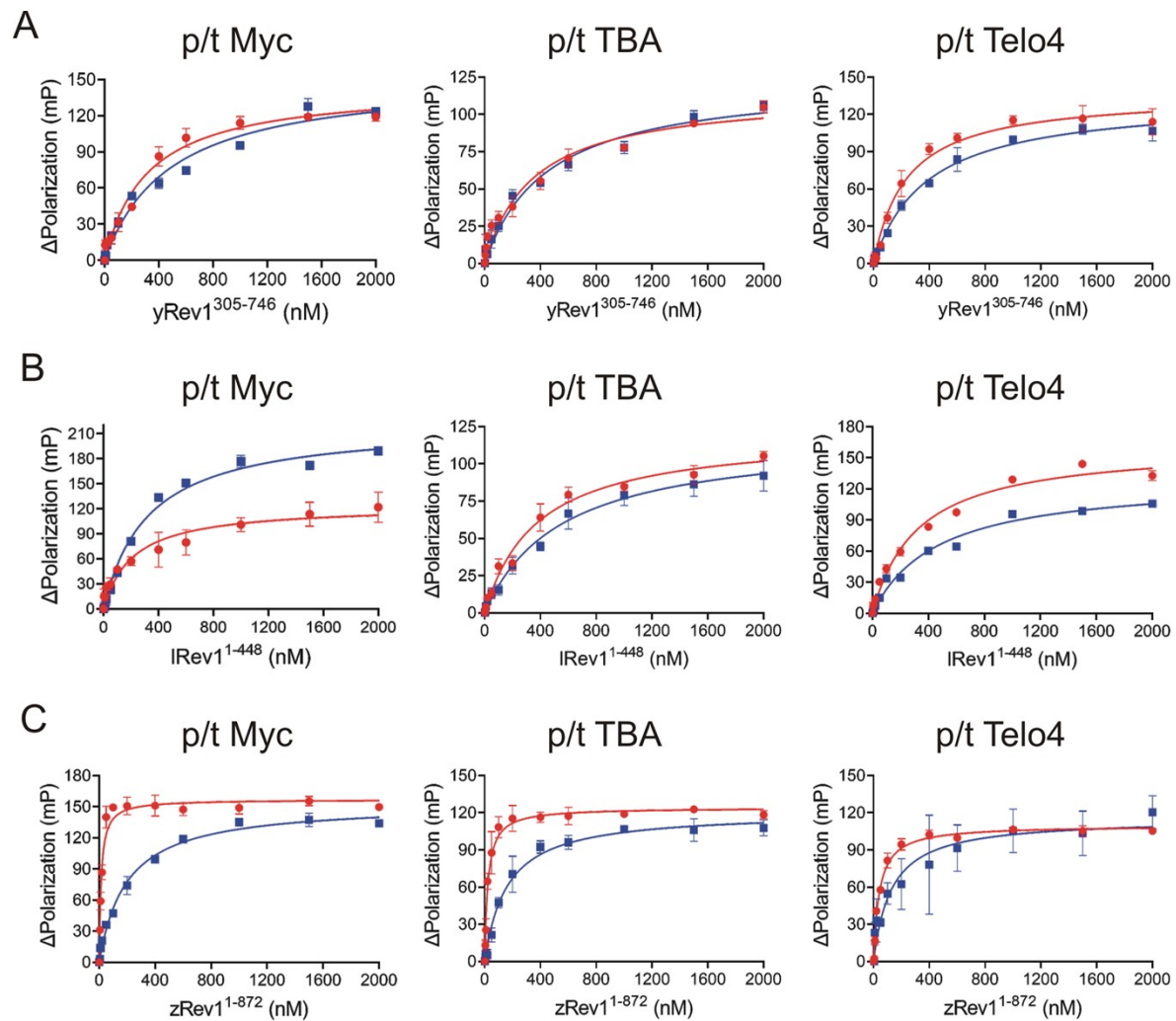


Figure S6. Binding curves for **A)** $yRev1^{305-746}$, **B)** $IRev1^{1-448}$ and **C)** $zRev1^{1-872}$ obtained using fluorescence polarization experiments with the indicated G4 (red) or non-G4 (blue) p/t DNA substrates in 100 mM KCl buffer. Proteins were titrated into a solution of each DNA (1 nM), and the change in fluorescence polarization at each protein concentration was measured and plotted as a function of concentration. The calculated $K_{D,DNA}$ values are listed in **Table 3**. The reported values represent the mean \pm std. dev. ($n=3$).

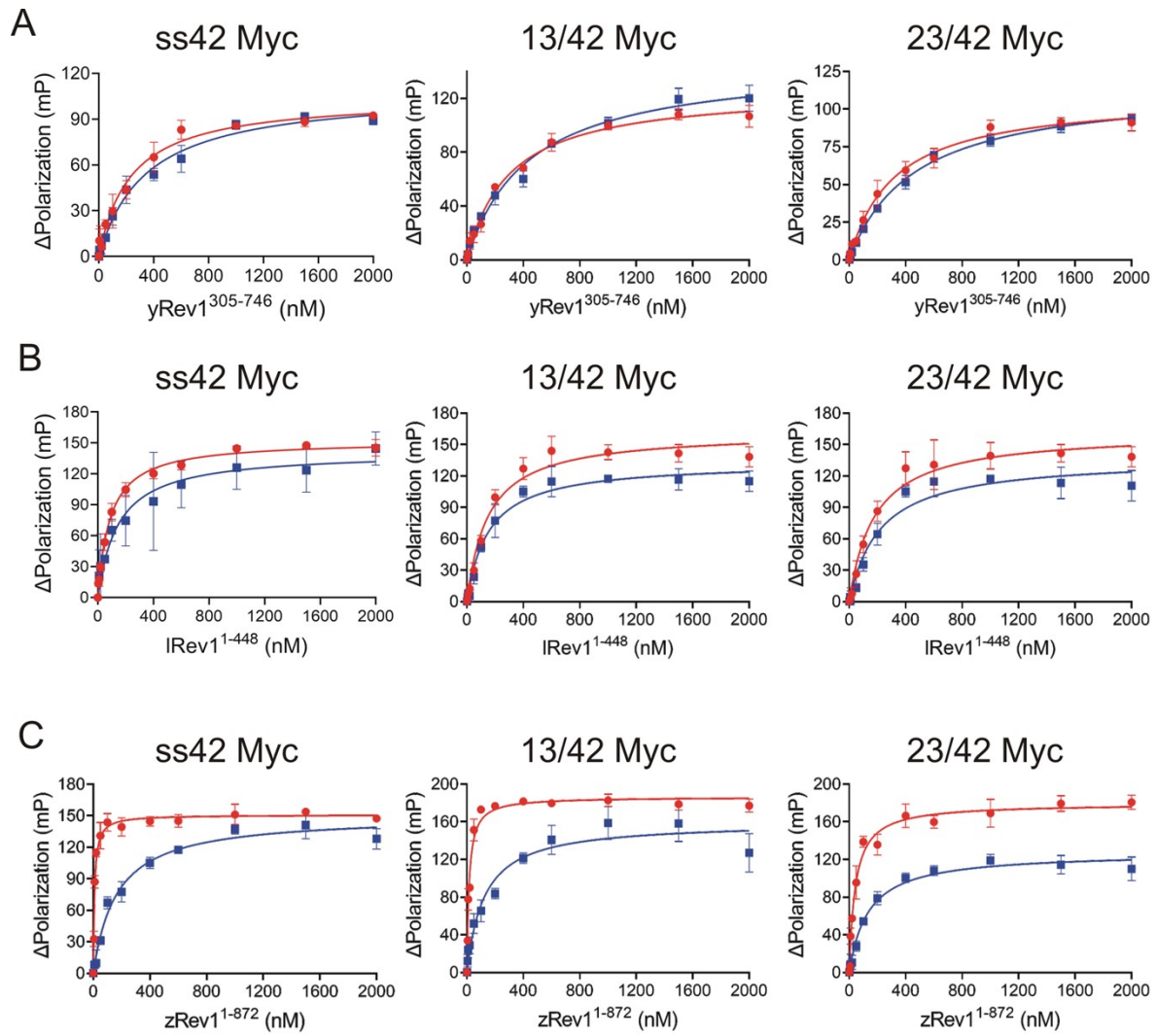


Figure S7. Binding curves for **A)** $yRev1^{305-746}$, **B)** $IRev1^{1-448}$ and **C)** $zRev1^{1-872}$ obtained using fluorescence polarization experiments with the indicated G4 (red) or non-G4 (blue) DNA substrates in 100 mM KCl buffer. Proteins were titrated into a solution of each DNA (1 nM), and the change in fluorescence polarization at each protein concentration was measured and plotted as a function of concentration. The calculated $K_{D,DNA}$ values are listed in **Table 4**. The reported values represent the mean \pm std. dev. ($n=3$).

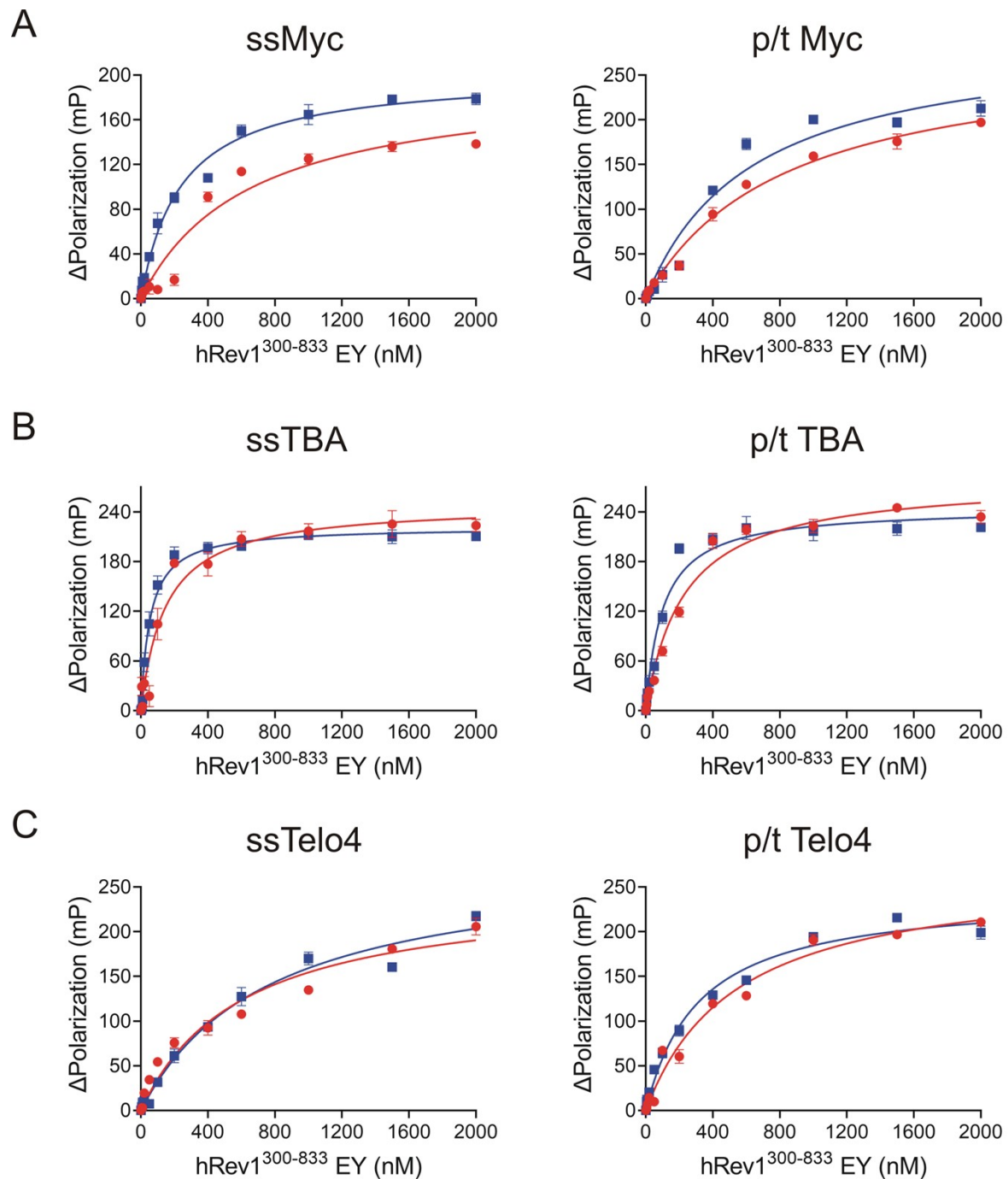


Figure S8. Binding curves for hRev1³⁰⁰⁻⁸³³ EY with the indicated G4 (red) or non-G4 (blue) ssDNA or p/t DNA substrates, obtained using fluorescence polarization experiments in 100 mM KCl buffer. Proteins were titrated into a solution of each DNA (1 nM), and the change in fluorescence polarization at each protein concentration was measured and plotted as a function of concentration. The calculated $K_{D,DNA}$ values are listed in **Table 5**. The reported values represent the mean \pm std. dev. (n=3).

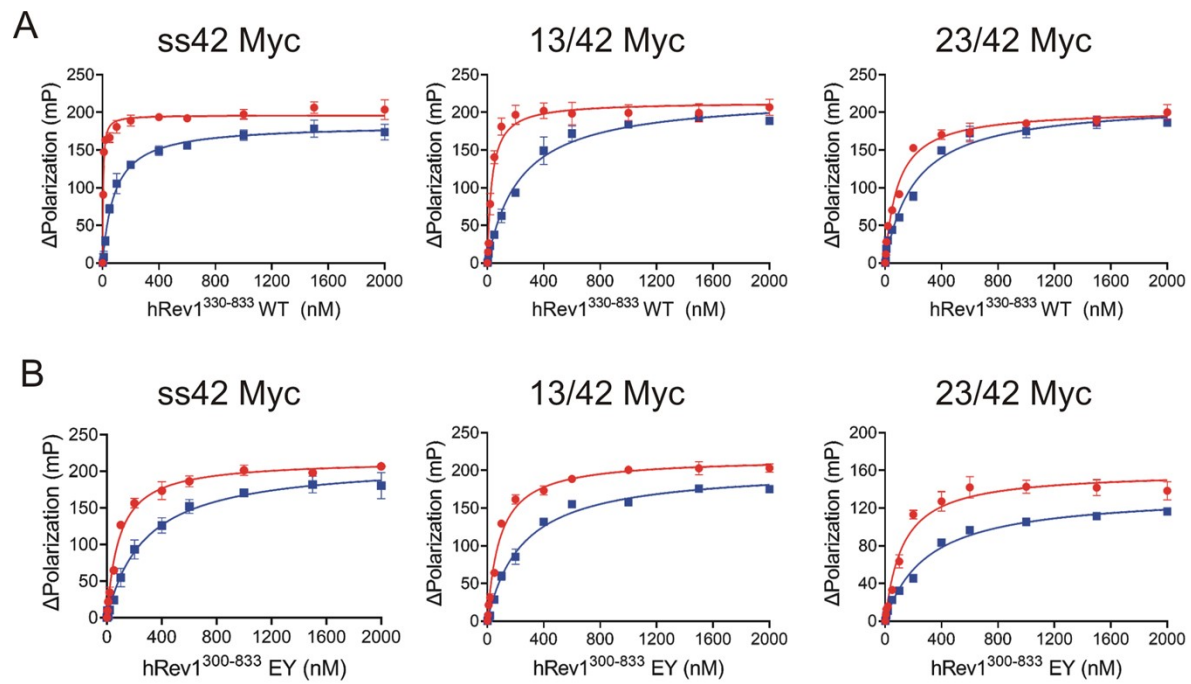


Figure S9. Binding curves for **A)** hRev1³³⁰⁻⁸³³ WT and **B)** hRev1³³⁰⁻⁸³³ EY with the indicated G4 (red) or non-G4 (blue) substrates, obtained using fluorescence polarization experiments in 100 mM KCl buffer. Proteins were titrated into a solution of each DNA (1 nM), and the change in fluorescence polarization at each protein concentration was measured and plotted as a function of concentration. The calculated $K_{D,DNA}$ values are listed in **Table 6**. The reported values represent the mean \pm std. dev. (n=3).

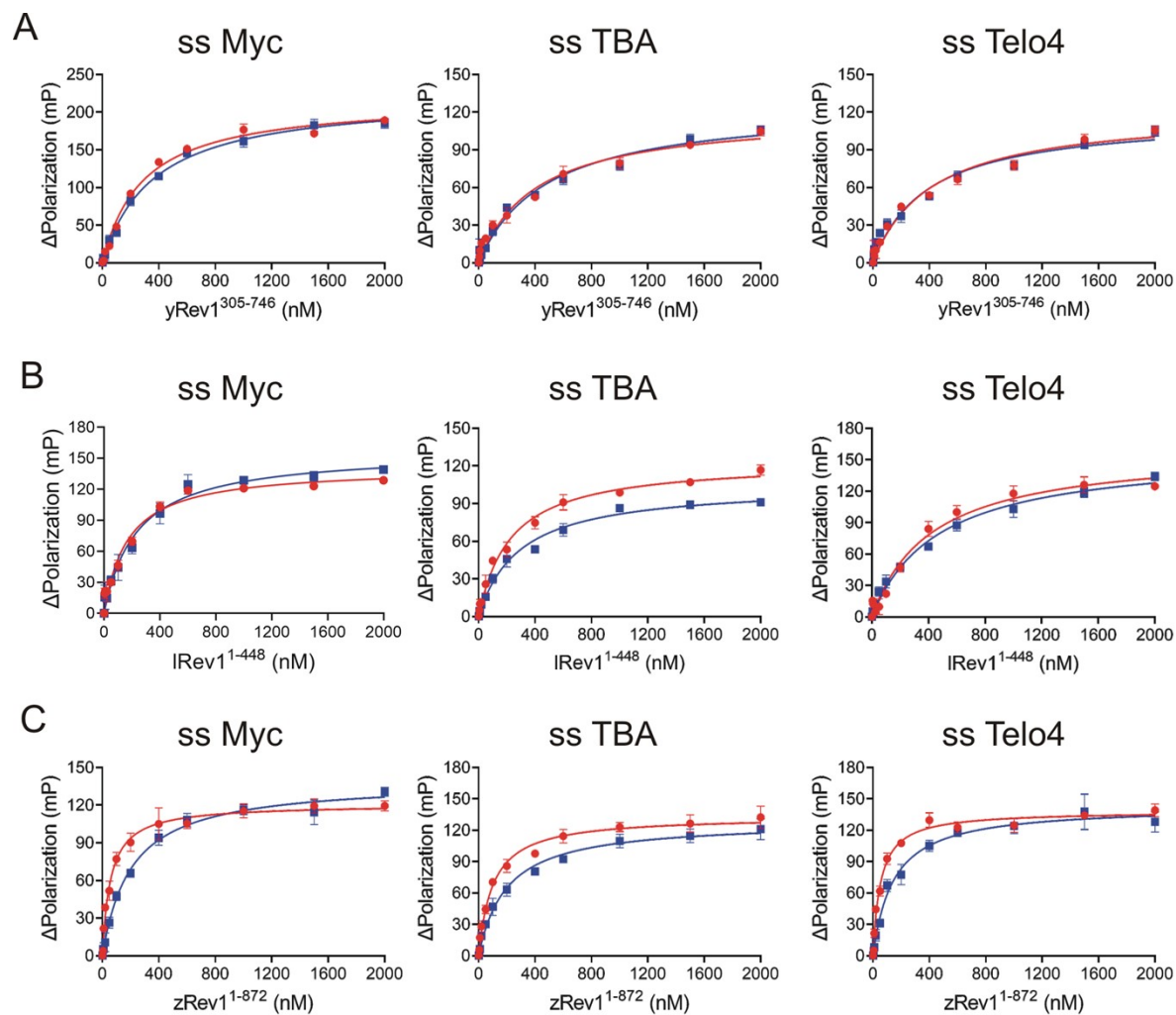


Figure S10. Binding curves for **A)** $yRev1^{305-746}$, **B)** $IRev1^{1-448}$ and **C)** $zRev1^{1-872}$ obtained using fluorescence polarization experiments with the indicated G4 (red) or non-G4 (blue) ssDNA substrates in 100 mM LiCl buffer. Proteins were titrated into a solution of each DNA (1 nM), and the change in fluorescence polarization at each protein concentration was measured and plotted as a function of concentration. The calculated $K_{D,DNA}$ values are listed in **Table S1**. The reported values represent the mean \pm std. dev. ($n=3$).

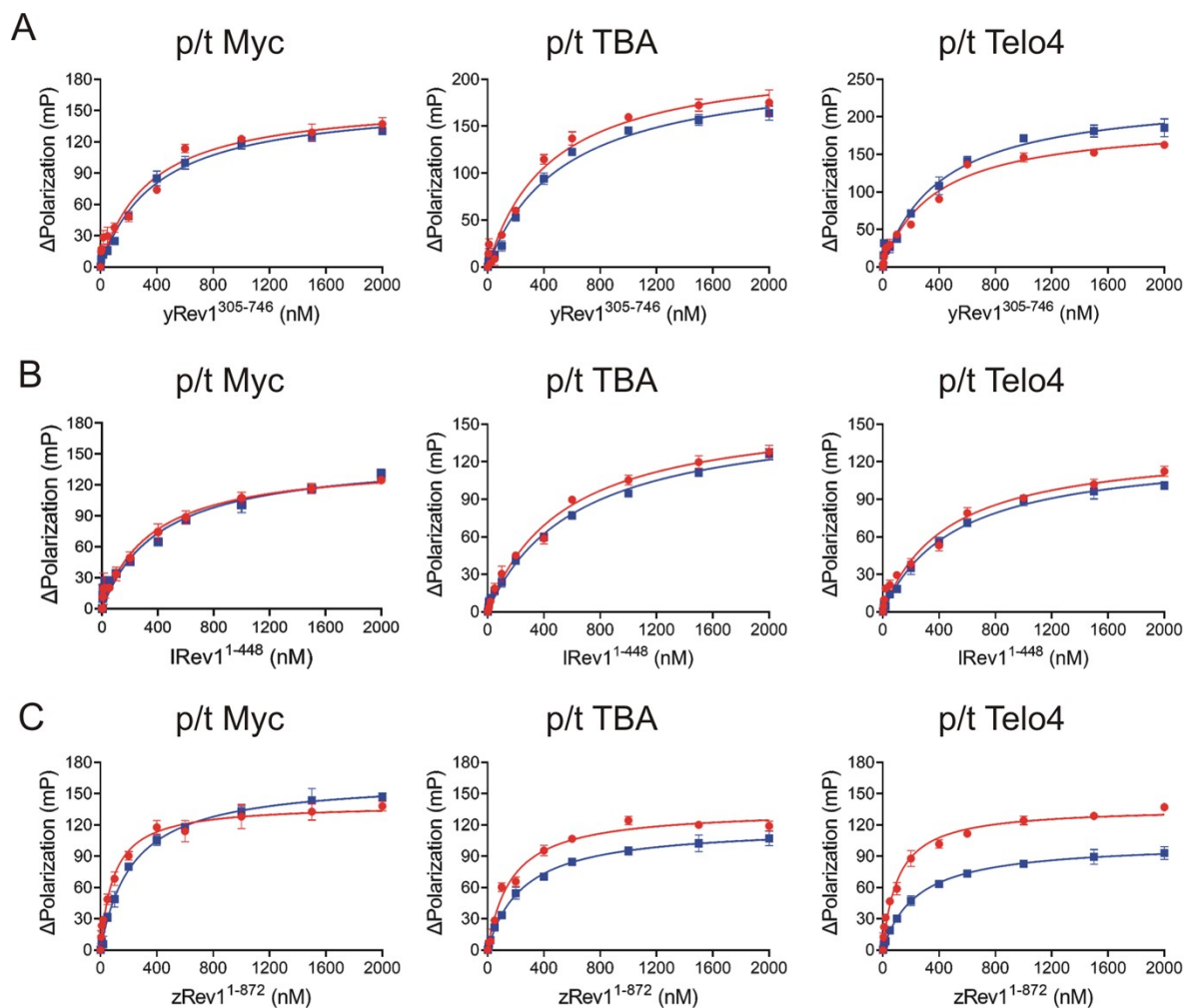


Figure S11. Binding curves for **A)** $yRev1^{305-746}$, **B)** $IRev1^{1-448}$ and **C)** $zRev1^{1-872}$ obtained using fluorescence polarization experiments with the indicated G4 (red) or non-G4 (blue) p/t DNA substrates in 100 mM LiCl buffer. Proteins were titrated into a solution of each DNA (1 nM), and the change in fluorescence polarization at each protein concentration was measured and plotted as a function of concentration. The calculated $K_{D,DNA}$ values are listed in **Table S2**. The reported values represent the mean \pm std. dev. ($n=3$).

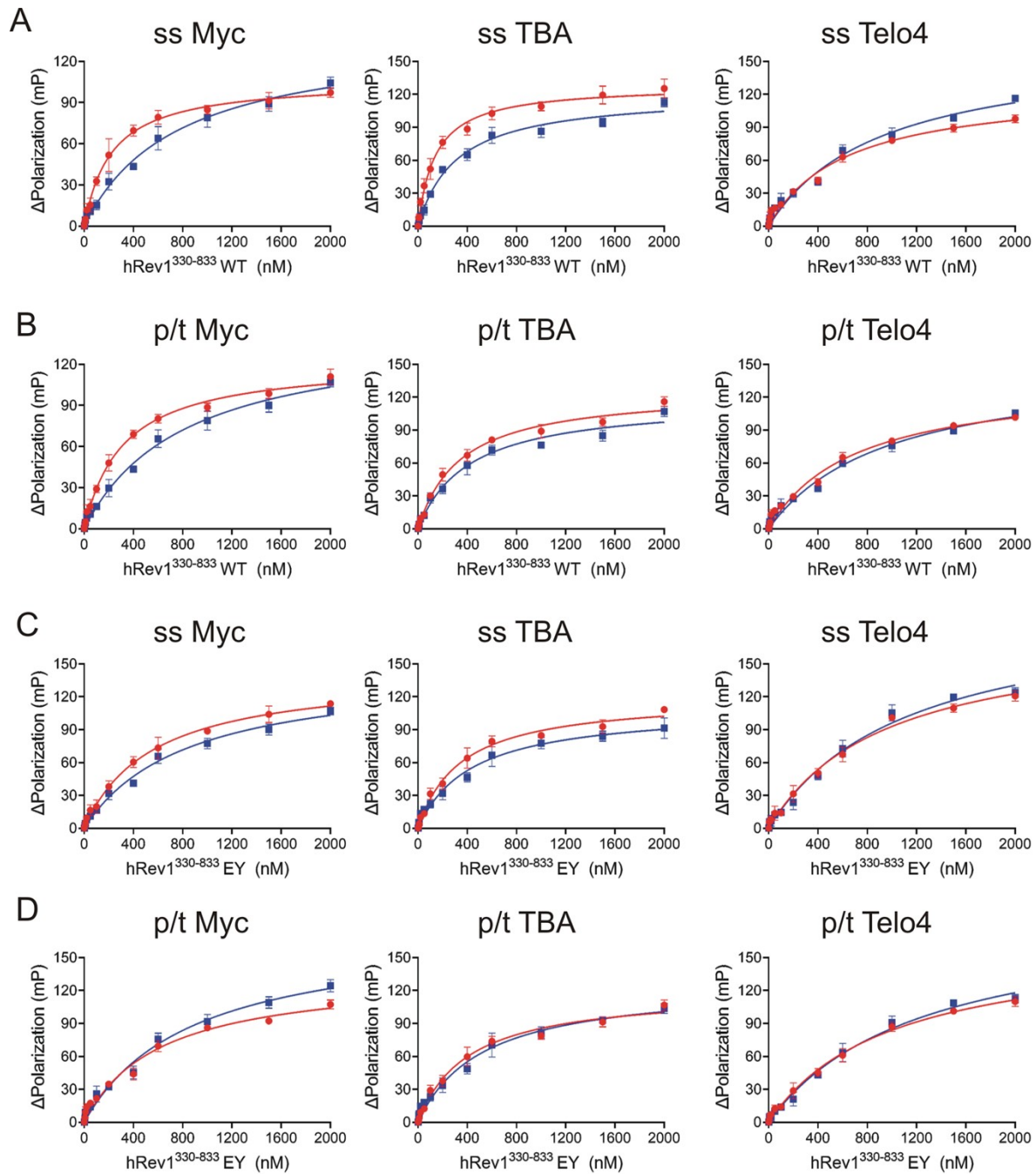


Figure S12. Binding curves for hRev1³³⁰⁻⁸³³ WT (panels **A** and **B**) and hRev1³³⁰⁻⁸³³ EY (panels **C** and **D**) with the indicated G4 (red) or non-G4 (blue) ssDNA or p/t DNA substrates, obtained using fluorescence polarization experiments in 100 mM LiCl buffer. Proteins were titrated into a solution of each DNA (1 nM), and the change in fluorescence polarization at each protein concentration was measured and plotted as a function of concentration. The calculated $K_{D,DNA}$ values are listed in **Table S3**. The reported values represent the mean \pm std. dev. (n=3).